Journal of Structural Geology, Vol. 7, No. 2, pp. 145 to 160, 1985
Printed in Great Britain

0191-8141/85 $03.00 + 0.00

Structural evolution of a nappe complex, southern Vanoise massif, French Penninic Alps

J. P. PLATT

Department of Geology and Mineralogy, Oxford University, Parks Road, Oxford OX1 3PR, U.K.

and

G. S. LISTER*

Institute of Earth Sciences, University of Utrecht, P.O. Box 80.021, 3508TA Utrecht, The Netherlands

(*Received* 29 *March* 1984; *accepted in revised form* 19 *September* 1984)

Abstract—The Arpont–Parrachée region in the southern Vanoise massif comprises a stack of minor fold- and thrust-nappes that were emplaced during subduction and closure of the Piémont ocean basin in Late Cretaceous to Eocene time. The stack includes the Arpont nappe, composed mainly of pre-Permian schist metamorphosed to blueschist facies early in the Alpine history, and several sheets of Permian to Eocene metasedimentary rocks. Nappe formation, recumbent folding, and associated ductile deformation postdated the high-pressure metamorphic peak, and probably involved translation to the northwest. The rocks were then refolded by large- and small-scale folds trending roughly E–W. These deformational events were accompanied by a decrease in metamorphic pressure, indicating uplift. They were followed by regional greenschist-facies metamorphism, which caused breakdown of high-pressure parageneses, annealing of microstructures, and widespread growth of albite porphyroblasts. The entire nappe pile was then refolded by large- and small-scale folds overturned towards the southeast. Reorientation of small-scale structures with increasing strain by this event indicates a large component of ESE-directed shear, which culminated in the formation of anastomosing ductile shear-zones.

INTRODUCTION

THE southern Vanoise massif (Fig. 1) lies in the Pennine Zone—a composite tectonic assemblage in the core of the Alps, formed during the subduction and ultimate closure of one or more small ocean basins during late Cretaceous to end-Eocene time (Milnes 1978, Frisch 1979, Homewood *et al.* 1980, Tricart 1984). Together with the weakly metamorphosed Carboniferous and Permian sediments of the Zone Houillère, the massif constitutes a southern continuation of the Grand Saint Bernard nappe complex in the Swiss Alps. These terrains probably formed part of a semi-independent Briançonnais block during Jurassic to Eocene time (Debelmas & Lemoine 1970, Frisch 1979, Trümpy 1980). They are now regionally overlain by the Piémont nappes, comprising metamorphosed calcareous sediments (Schistes Lustrés) and ophiolitic rocks from the Piémont ocean basin. The Vanoise massif itself is made up of the pre-Permian Arpont schist and Permian to Eocene metasedimentary rocks. Three Mesozoic facies series are distinguished by Ellenberger (1958) and Raoult (1980), who assign the sequence in the area described here to the Grande Motte series, characterized by an unusually thick sequence of Liassic siliceous limestones. Ellenberger (1958) regarded this series as forming a nappe derived from the eastern margin of the Briançonnais platform, adjacent to the Piémont basin.

*Present address: Bureau of Mineral Resources, P.O. Box 378, Canberra City, Australia.

The Vanoise is a region of spectacular nappe tectonics, and by a fortuitous combination of circumstances provides an ideal area for detailed study of the structural and metamorphic evolution of Penninic nappes. Firstly, the Permian to Eocene 'cover' sequences of the area are, broadly, in the Briançonnais platform facies (Trümpy 1960, Debelmas & Lemoine 1970, Debelmas 1974, 1980) and hence comprise easily recognizable and mappable lithostratigraphic units. These have been dated palaeontologically by the monumental studies of Ellenberger (1958), so that their primary sequence and younging are known. This allows unravelling of structures that might not be discernible in areas dominated by the monotonous Schistes Lustrés facies, which lacks internal stratigraphy or fossils. Secondly, the area has been affected by high-pressure low-temperature metamorphism; and thirdly, the early metamorphic parageneses and textures have not been completely overprinted by later thermal events. The purpose of this paper is to provide a case-history documentation of the structural development of a small part of the southern Vanoise, around the mountain La Dent Parrachée, north of Modane in the Arc Valley. We believe that this is a key area, in that it allows us on the one hand to relate the structural development of the region to the microstructural and metamorphic history; and on the other hand it contains major structures that can be integrated into the larger-scale tectonics of this part of the Penninic Alps.

Tectonic syntheses of the area generally postulate two major tectonic events: the first involved the translation of major nappes towards the west, and the second caused 'retrocharriage', involving thrusting and folding

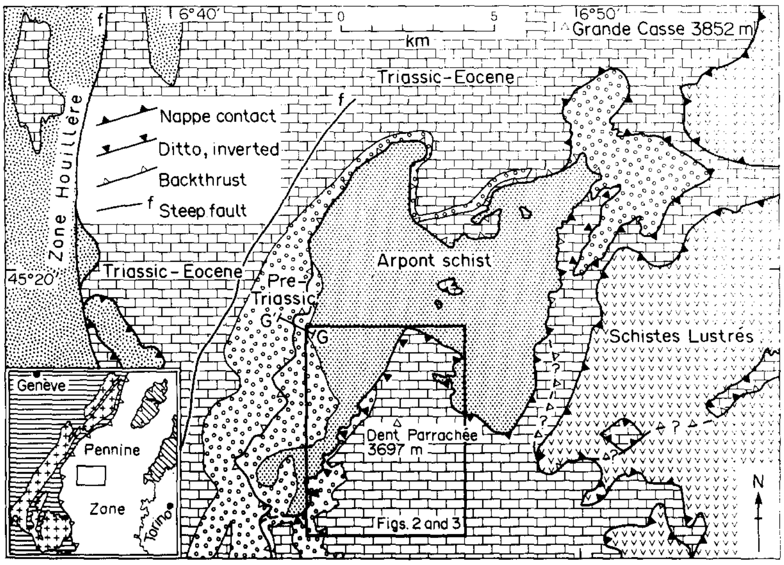

Fig. 1. Geological setting of the southern Vanoise massif. Arpont schist: pre-Permian metamorphic complex. Zone Houillère: low grade Carboniferous and Permian clastic metasedimentary rocks, and foliated metagranite (Gneiss du Sapey). Open circles, pre-Triassic metaclastic rocks of probable Permian age; bricks, Triassic to Eocene (Briançonnais facies); v-pattern, Schistes Lustrés. Inset: Western Alps. Horizontal lines, External Zone cover; crosses, external crystalline massifs; diagonal lines, Austro-Alpine and Southern Alpine domains.

back towards the east (e.g. Debelmas 1976, Debelmas & Kerckhove 1980, Tricart *et al.* 1977, Raoult 1980). Caby *et al.* (1978), however, suggested that the E-directed thrusting was related to a W-dipping subduction zone, that it was accompanied by high P/T ratio metamorphism, and was followed by renewed westward thrusting that emplaced the Austro-Alpine nappes. We present evidence here that the structure of the southern Vanoise can be explained in terms of an early phase of NW-directed nappe transport that post-dated the high-pressure metamorphic peak, a phase of E–W folding about roughly E–W-trending axes accompanied and followed by greenschist-facies metamorphism, followed by ESE directed thrusting and folding under low-grade conditions.

THE NAPPE PILE

The Arpont nappe

The Arpont nappe is the lowest of the tectonic units that we distinguish in the southern Vanoise (Figs. 2 and 3). It includes the Arpont schist, which is a large body of metasedimentary and metabasic rocks metamorphosed under amphibolite-facies conditions in Palaeozoic time (Bocquet 1974b). The lower contact of the nappe is not seen, but an inverted lower limb is visible where it has been turned up on end by backfolding on the western side of the massif. This can be seen for example west of the Pointe de Labby (Fig. 4c) and in the Cirque du Génépy (Fig. 5b, UTM 3213,0208 on map-sheet Modane 3–4), where an inverted sequence of pre-Triassic conglomerate and metaclastic rocks lies in nonconformable contact with the schist. The Arpont nappe therefore appears to contain the disrupted remnant of a major recumbent fold. Its upper surface is in tectonic contact with the overlying nappes.

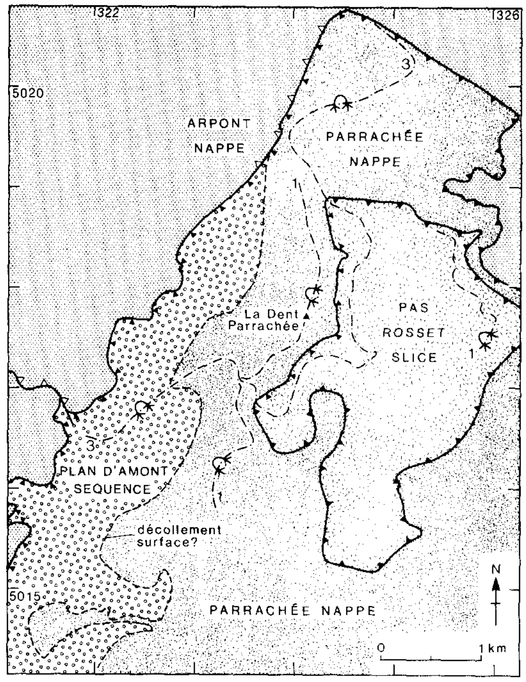

Fig. 2. Tectonic sketch-map of the area around La Dent Parrachée, to show the principal tectonic elements. Structures are numbered by age. See Fig. 3 for structural symbols. Marginal numbers are UTM coordinates.

Fig. 3. Simplified structural map of the region around La Dent Parrachée. Superficial deposits have been omitted. Spot heights in metres. L_1, glaucophane lineation; L_2 and L_3, second and third phase minor fold-axes and intersection lineations; L_e, D_3 elongation lineation; ecc, extensional crenulation cleavage. Marginal numbers are UTM coordinates.

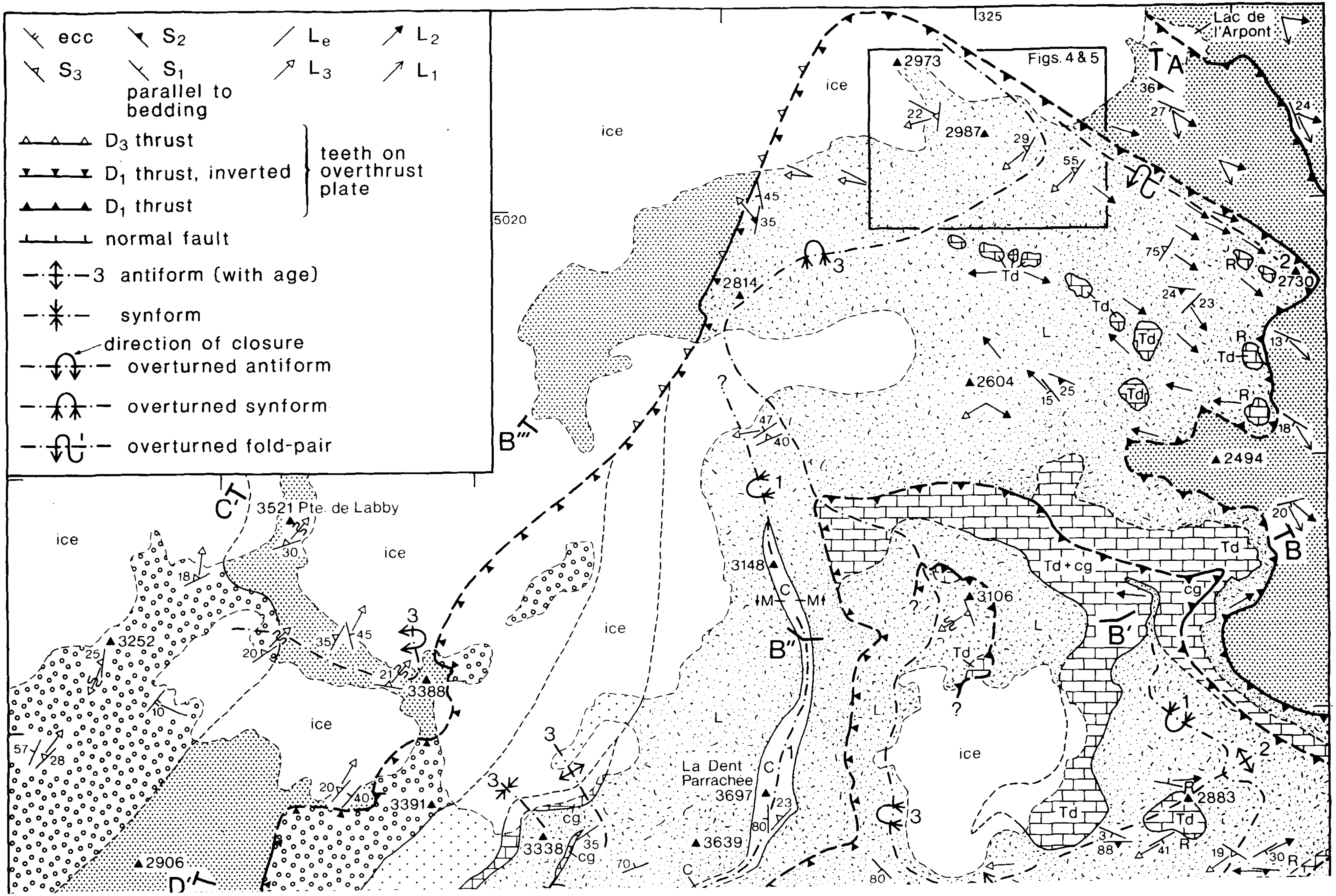
ecc
S2
Le
L2
S3
S1 parallel to bedding
L3
L1
D3 thrust
D1 thrust, inverted
D1 thrust
teeth on overthrust plate
normal fault
3 antiform (with age)
synform
direction of closure
overturned antiform
overturned synform
overturned fold-pair
Figs. 4 & 5
Lac de l'Arpont
325
5020
ice
3521 Pte. de Labby
La Dent Parrachée 3697
2973
2987
2814
2604
2494
2730
3148
3106
3252
3388
3391
3338
3639
2883
2906
Td
Td + cg
cg
A
B
B'
B''
B'''
C'
D'

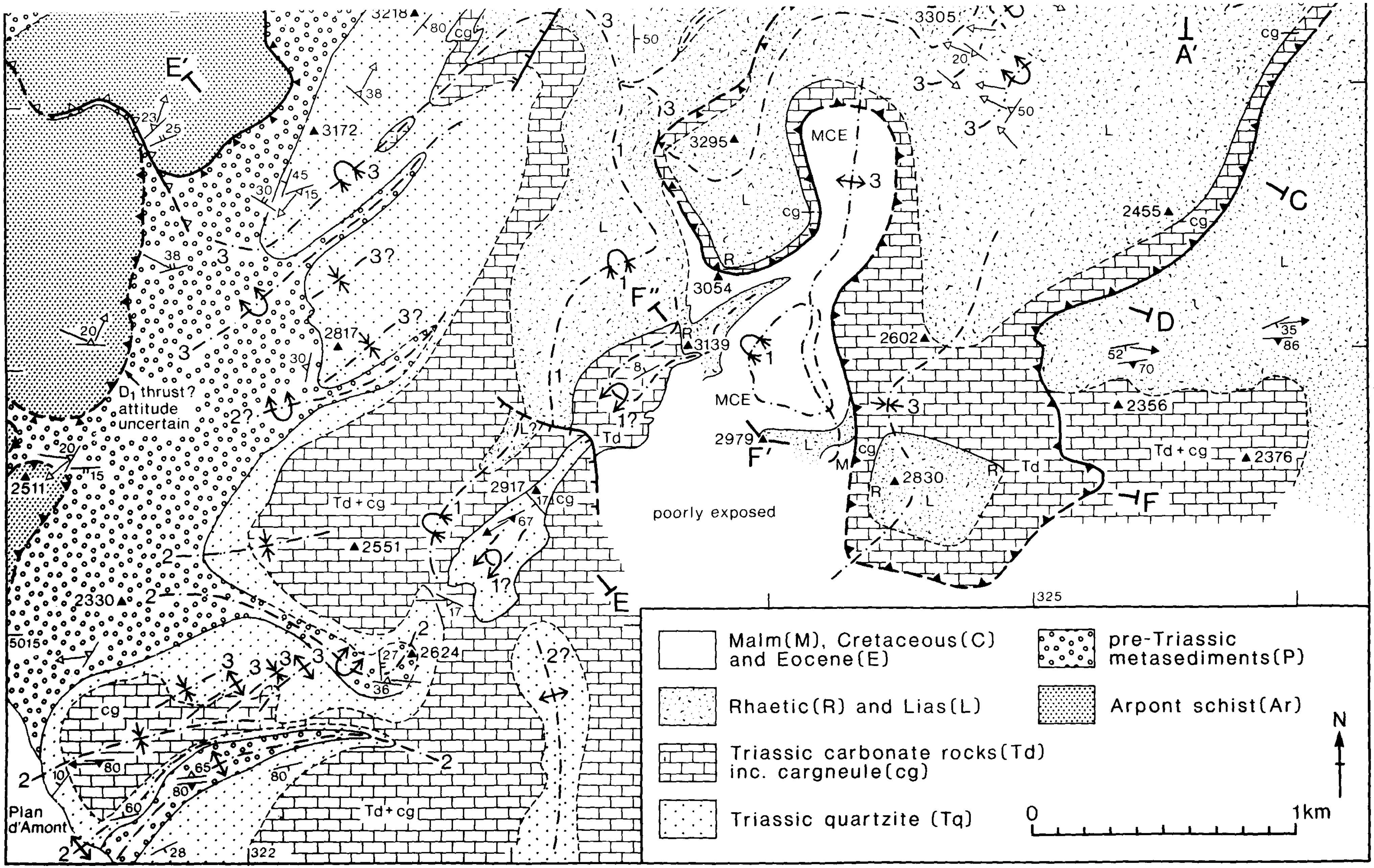

Malm(M), Cretaceous(C) and Eocene(E)
Rhaetic(R) and Lias(L)
Triassic carbonate rocks(Td) inc. cargneule(cg)
Triassic quartzite (Tq)
pre-Triassic metasediments(P)
Arpont schist(Ar)
0
1km
N
poorly exposed
D1 thrust? attitude uncertain
Plan d'Amont
MCE
Td + cg
E'
A'
C
D
E
F
F'
F''
3218
3172
2817
2511
2330
2551
2624
2917
3054
3139
2979
3295
3305
2602
2830
2455
2356
2376
5015
322
325

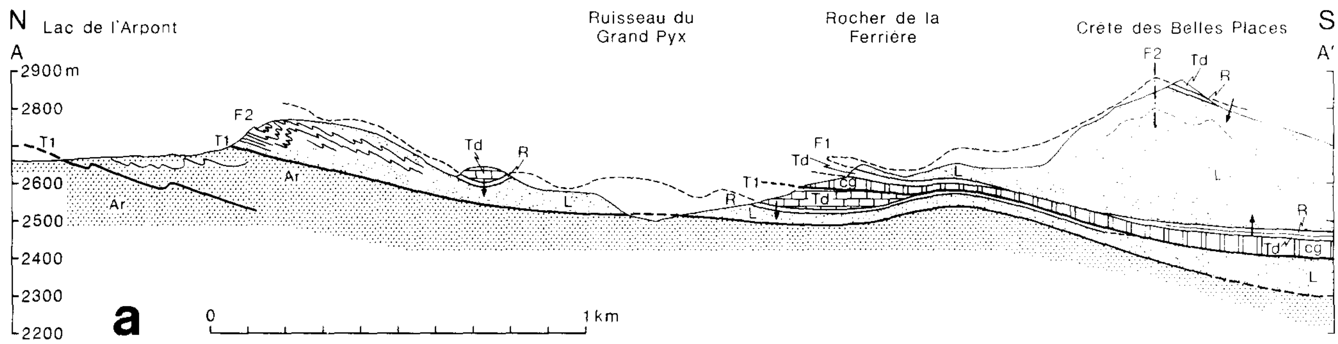

Fig. 4(a). Caption overleaf.

Permo-Triassic sequence of Plan d'Amont

West and south of La Dent Parrachée (Fig. 3), the Arpont schist is tectonically overlain by and interleaved with a variety of pre-Triassic rocks, including coarse-grained metasandstone and metaconglomerate, green chlorite–albite schist derived from mafic volcanic rocks, and pale green quartz–phengite schist. The latter passes with apparent conformity into pure white quartzite of assumed Triassic age (Ellengberger 1966). Both the upper and lower contacts of this sequence appear to be tectonic, and we show it as a separate unit on the tectonic map (Fig. 2). The lower contact (with the Arpont schist) is marked by a zone of strongly foliated phengite schist, and lithological units in the Permo-Triassic sequence are cut off against this contact (Figs. 3 and 4). The upper surface of the quartzite is overlain by a zone of cargneule containing blocks of Triassic dolomite, which separate it from Liassic limestone. Cargneule is a general term covering a variety of foliated or unfoliated calcareous or dolomitic breccias. It is commonly associated with gypsum, and probably forms along evaporite layers in the Triassic carbonate sequence. These layers have in many cases acted as décollement surfaces. The brecciation may be partly tectonic, or due to solution and reaction of dolomite with gypsiferous fluids, or both. The presence of cargneule along the upper contact of the quartzite, and the absence of a normal sequence of Triassic carbonate rocks, suggests that this contact is also tectonic. Displacement need not have been large, however, in which case the sequence can be regarded as part of the overlying Parrachée nappe, described below.

The Parrachée nappe and Pas Rosset slice

The Parrachée nappe is a major isoclinal syncline bounded by faults above and below (Figs. 2–4). The stratigraphic sequence in the Parrachée and related units is briefly summarized in Table 1. No attempt has been made to estimate original thicknesses, in view of the complicated history of penetrative deformation. West and southwest of La Dent Parrachée, the lower (right-way-up) limb of the nappe lies on the Triassic quartzite of the Plan d'Amont area, as described above. To the north and east, however, the normal limb is missing, and the inverted limb lies with an obvious tectonic contact on the Arpont schist (Figs. 3 and 4a). The Parrachée nappe is overlain by the Pas Rosset slice, another isoclinal syncline comprising Triassic and Liassic rocks identical to those in the Parrachée nappe. Right-way-up rocks of the Pas Rosset slice commonly lie on inverted rocks of the Parrachée nappe (Figs. 4b & c), so the fault contact may have replaced an original recumbent anticline linking the two structures. Taken together, the two units probably correspond to the Grand Motte nappe of Ellenberger (1958).

METAMORPHISM

The Arpont schist contains evidence of a prolonged and complicated metamorphic history, involving pre-Alpine amphibolite-facies metamorphism, a relatively early Alpine blueschist-facies event, followed by greenschist-facies metamorphism characterized by growth of albite and green biotite (Bocquet *et al.* 1974, Desmons 1977, Goffé 1977, Platt & Lister 1978). Platt & Lister (1985) show that the high-pressure peak predates all mesoscopically recognizable deformational events in the area, and was followed by deformation presumably associated with the emplacement of the Arpont nappe, under conditions of decreasing pressure. The thermal

Table 1. Simplified stratigraphy of the Parrachée nappe and related units

Eocene (E)	Black calcareous slate
Late Cretaceous to Palaeocene (C)	Yellow–green marble with flecks of chlorite and white mica
Late Jurassic (M)	Pure light grey to white marble (Malm)
Early Jurassic (L)	Grey platy limestone, with thin yellow-weathering siliceous interlayers, black calcite nodules, and sedimentary breccia horizons containing calcareous and dolomitic debris (Lias).
Rhaetic (R)	A thin unit of black shale, greenish-yellow dolomite, and discontinuous bodies of grey shelly or coralline limestone.
Middle to Late Triassic (Td)	Grey thick-bedded limestone and cream weathering massive dolomite, commonly largely altered to cargneule.
Early Triassic (Tq)	Massive white quartzite, locally cross-bedded. Age not precisely determined.
"Permian" (P)	Undated metaconglomerate, micaceous metasandstone, chlorite–albite schist, and quartz–phengite schist.

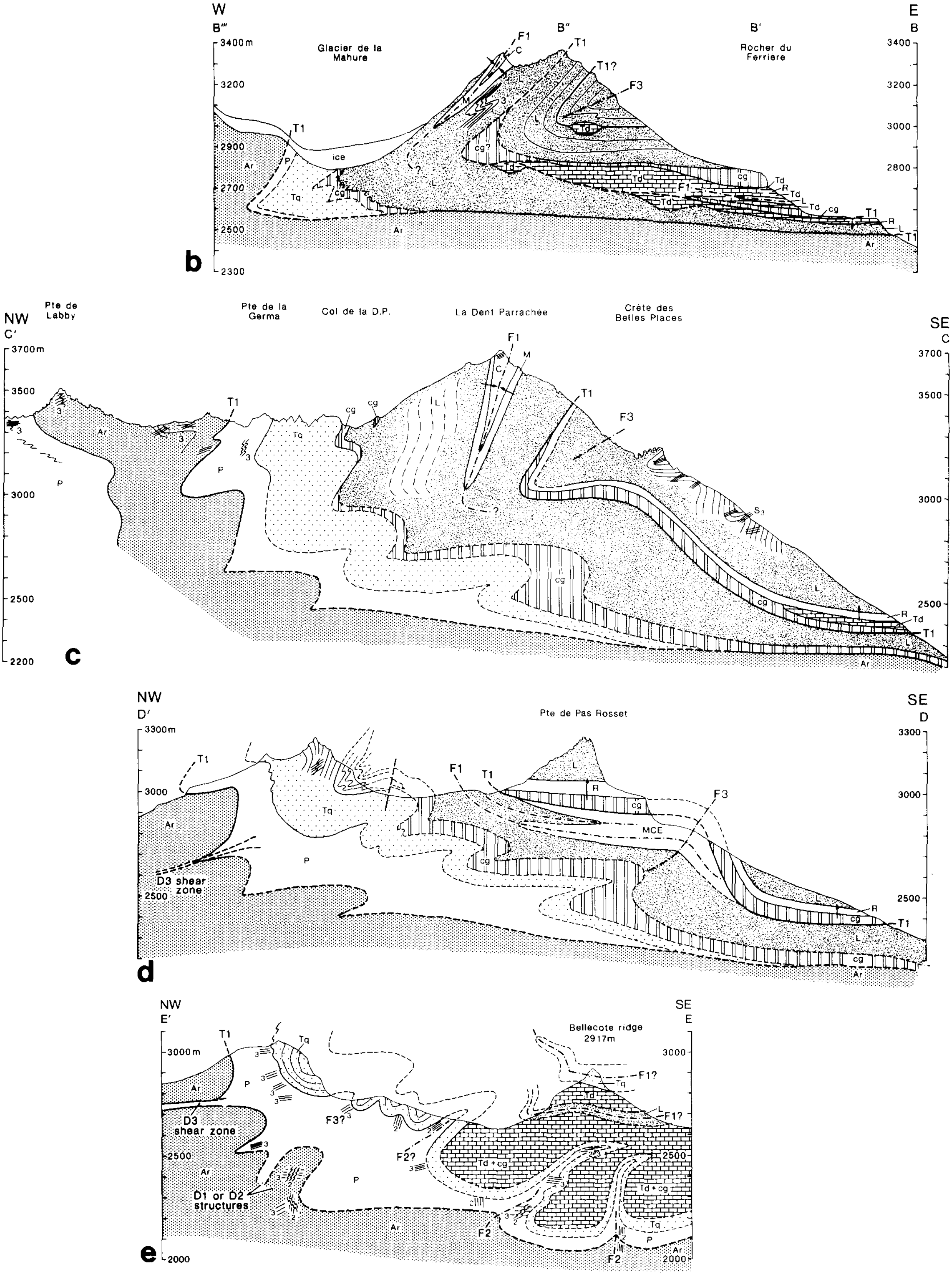

Fig. 4. Structural sections: for location see Fig. 3. T_1, etc., thrusts, with age; F_1, etc., major folds. Small-scale structures numbered by age. Stratigraphic abbreviations as in Fig. 3 and Table 1. Arrows show stratigraphic younging determined from sequences of at least three palaeontologically dated units. Details of structure at depth (dashed lines) are speculative, but the essential geometry is constrained by surface observations. In section EE′ the D_1 age shown for the recumbent folds in the Bellecôte ridge is uncertain. An alternative possibility is that they are D_2 folds rotated into a recumbent position during D_3.

peak represented by growth of chlorite and albite postdates nappe emplacement, but predates the SE-directed folding. We suggest that this thermal peak correlates roughly with the Lepontine metamorphic event in the central Alps, which has been dated at around 38 Ma (Frey *et al.* 1974).

Metamorphic evidence from the other nappes in the area is far more scanty. The Permo-Triassic rocks of Plan d'Amont show no evidence for the early *HP/LT* metamorphic history revealed by the Arpont nappe. Mineral assemblages are those of the greenschist facies: chlorite + albite ± epidote ± actinolite ± carbonate in mafic rocks, and quartz + phengitic white mica ± chlorite ± albite ± carbonate ± magnetite ± tourmaline in metasedimentary rocks. Chloritoid occurs in some plagioclase-free rocks. The carbonate rocks of the Parrachée and Pas Rosset nappes, on the other hand, do contain relics of a high *P/T* ratio event: blue amphibole (mainly crossite, Bocquet 1974a), and pseudomorphs of lawsonite (Ellenberger 1960). These appear to have grown early in the deformational history. Fe,Mg-carpholite has also been reported from Mesozoic rocks in the western Vanoise (Goffé *et al.* 1973, Goffé 1982). The dominant mineral assemblages in these nappes formed during the greenschist-facies event, however, and include carbonate minerals, quartz, white mica, Mg-chlorite, and porphyroblasts of albite. Albite growth predates the SE-directed folding.

DEFORMATION HISTORY

We recognize three groups of structures in the Arpont–Parrachée area, which we refer to as D_1, D_2 and D_3. We believe that this analytical approach is an essential first step to achieve an understanding of the tectonics of the area (see Platt & Lister 1985, for a summary of our working methods and philosophy). The relationships of these sets of small-scale structures to each other and to the large-scale tectonic events are discussed in the Tectonic Synthesis. The structures described below are illustrated in the structural maps (Figs. 3, 6 and 7) and sections (Figs. 4 and 5), and some of the orientation data are summarized on equal-area plots (Fig. 8).

Early structures

In the Arpont nappe, tight folds, a regionally flat-lying glaucophane–mica schistosity S_1 and a NW-trending glaucophane lineation L_1 (Figs. 3 and 8), are associated with the later stages of blueschist-facies metamorphism, after the high-pressure peak. These are commonly the most pronounced mesoscopically visible fabrics, although earlier fabrics of probable pre-Alpine age are locally preserved. The D_1 structures are probably broadly related to the formation of the major recumbent folds and thrusts that define the nappes. The regionally consistent mineral lineation represents the finite elongation direction during this deformation (D_1), and may indicate the approximate transport direction during nappe emplacement. In the north of the area the Arpont nappe is cut by a thrust (Figs. 3 and 4a), marked by a zone of Permian phyllite, with a displacement of several kilometres. It cuts up through the schist towards the north, suggesting displacement in roughly this direction (Platt & Lister 1985). Similar thrusts may be present in the southwest of the area, but these have been heavily overprinted by D_2 and D_3, and the age and nature of these structures is uncertain.

Early structures in the Parrachée nappe include small-scale isoclinal folds and a layer-parallel schistosity. Medium- to large-scale isoclinal folds are indicated by inversions in the stratigraphy, particularly around the summit of La Dent Parrachée (Figs. 4b & c, and 9a & b) and around the Pointe de Bellecôte (Fig. 5a). These structures lie in the axial zone of the major syncline in the Parrachée nappe, and were probably associated with some stage in the formation of the nappe structure. We have not been able to identify and measure fold axes and lineations. The schistosity is defined in part by oriented sheet silicates, but it has been considerably modified by later events. Locally, in Rhaetic limestone, we have observed what appears to be a pressure-solution cleavage defined by anastomosing seams of carbonaceous material (Fig. 9c), but this microstructure has been completely overprinted by grain-growth of calcite.

In view of the probable large displacement on the nappe contacts we cannot assume that the early structures formed at exactly the same time in each nappe. It is also true that the small-scale structures and fabrics cannot be unequivocally related to the formation of the nappes.

The nappe contacts are commonly marked by thick layers of cargneule: spectacular examples are the base of the Pas Rosset slice, and the base of the Schistes Lustrés nappe. Much of the cargneule is a disorganized breccia that provides no useful structural information, and outcrops are commonly covered by a false cargneule—recent talus that has been cemented by calcite and limonite deposited from ground-water channelled through the true cargneule. Substantial blocks of dolomite, up to several tens of metres thick, are distributed along the contacts, commonly in association with cargneule. These are presumably relics of the Triassic carbonate sequence that contained the evaporite horizons responsible for décollement and the formation of the cargneule.

Thin layers of calc-mylonite occur on some contacts, particularly where cargneule is not developed. Much of this mylonite is now coarse-grained marble: its high strain state is revealed by fine laminar banding, 'augen' of dolomite in a calcite matrix, and highly deformed primary clastic particles. The mylonite along the Arpont/Parrachée nappe contact near spot height 2730 m (UTM 3262,0198) has alternating coarse calcite and fine calcite/dolomite bands: the two phase mixture has presumably inhibited subsequent grain growth. It has a strong stretching lineation oriented about 105–120°, which probably indicates the movement direction, but there is evidence that this contact was reactivated as a décollement surface during D_2 (see below).

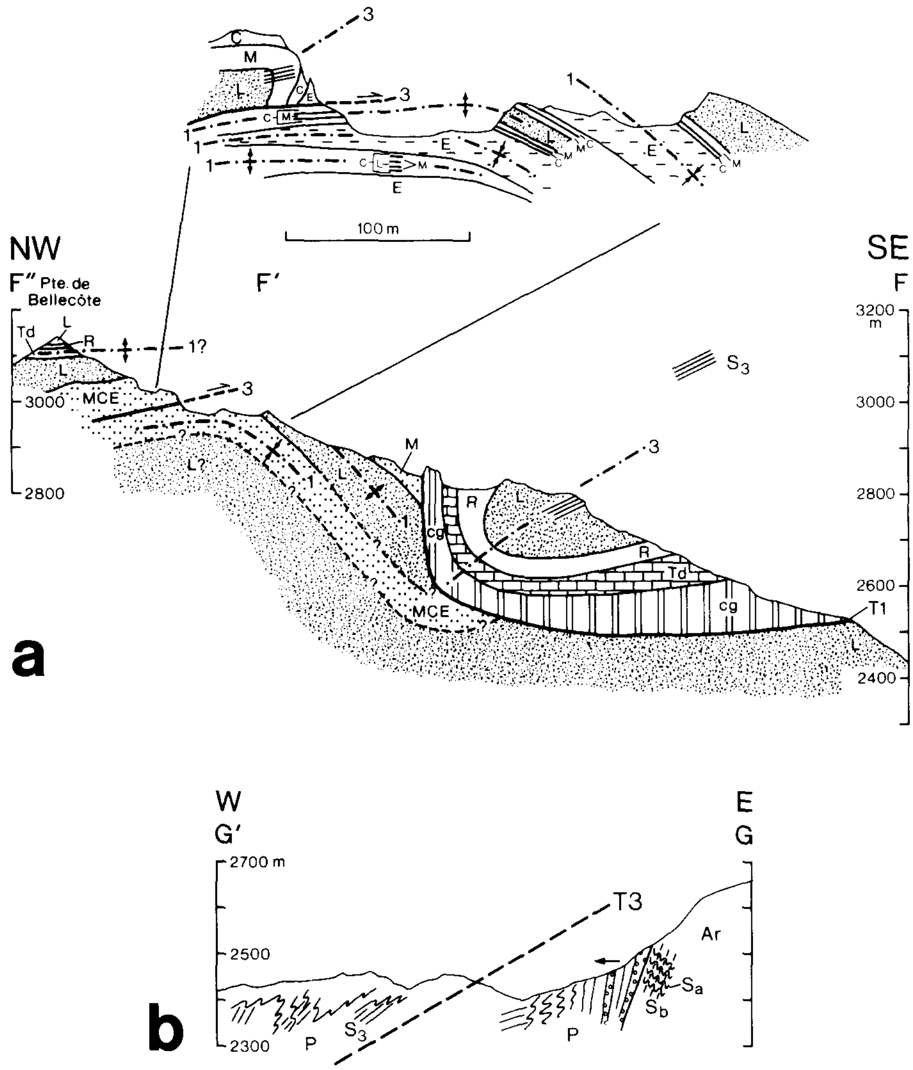

Fig. 5. Structural sections. (a) Section FF″ through the Pointe de Bellecôte, see Fig. 2 for location. Inset shows details of D_1 folds. (b) Section GG′ in the Cirque du Génépy (UTM 3213,0208, see Fig. 1). Open circles, basal conglomerate in pre-Triassic sediment sequence lying on Arpont schist. Younging determined from sedimentary structures. In the Arpont schist, S_a is probably a pre-Alpine foliation cut off by the unconformity; S_b is probably S_1 (Alpine).

D_2 *structures*

Variably oriented roughly E–W trending post-nappe folds with S-dipping to vertical axial planes can be recognized in all tectonic units. We call these structures D_2, but note that they did not necessarily all form at the same time, or for the same reasons. Large-scale non-cylindrical D_2 folds with an axial-plane differentiated crenulation cleavage affect the Permo-Triassic sequence of the Plan d'Amont area and the upper surface of the underlying Arpont nappe (Fig. 4e). These were initially upright structures with very open synforms and tightly pinched antiforms, but they have been variably deformed and reoriented by D_3. Their geometry appears to be a result of the contrast between the very weak Permian phyllite and the overlying strong Triassic quartzite and dolomite.

In Liassic limestone of the Parrachée nappe east of Le Petit Mont (Figs. 4a, 6 and 7) small-scale highly cylindrical ESE-trending D_2 folds are N-vergent with S-dipping axial planes (Fig. 8). These folds do not deform the contact between the Arpont and Parrachée nappes, which therefore probably acted as a décollement surface during D_2. At (3256,0191) the limestone has been completely detached from the Arpont schist beneath a cascade of metre-scale N-vergent D_2 folds, and the void is filled with several metres of carbonate–albite–haematite rock. Identical D_2 folds within the Arpont nappe, however, fold the internal D_1 thrust. An axial-plane foliation S_2 has been produced by crenulation of S_1, and in carbonate rocks S_2 is marked by differentiation bands of quartz and calcite 1–2 mm wide (Fig. 10c). This points to an important role for diffusional mass-transfer (pressure-solution) of the two minerals at significantly different rates. The association of the quartz with relatively immobile phases such as white mica and carbonaceous material suggests that calcite was the more mobile of the two. A strong roughly E–W trending intersection or crenulation lineation L_2 is widely developed in all rock-types (Fig. 3) and is a useful indicator of this set of structures.

In areas of relatively low D_2 strain, such as Plan

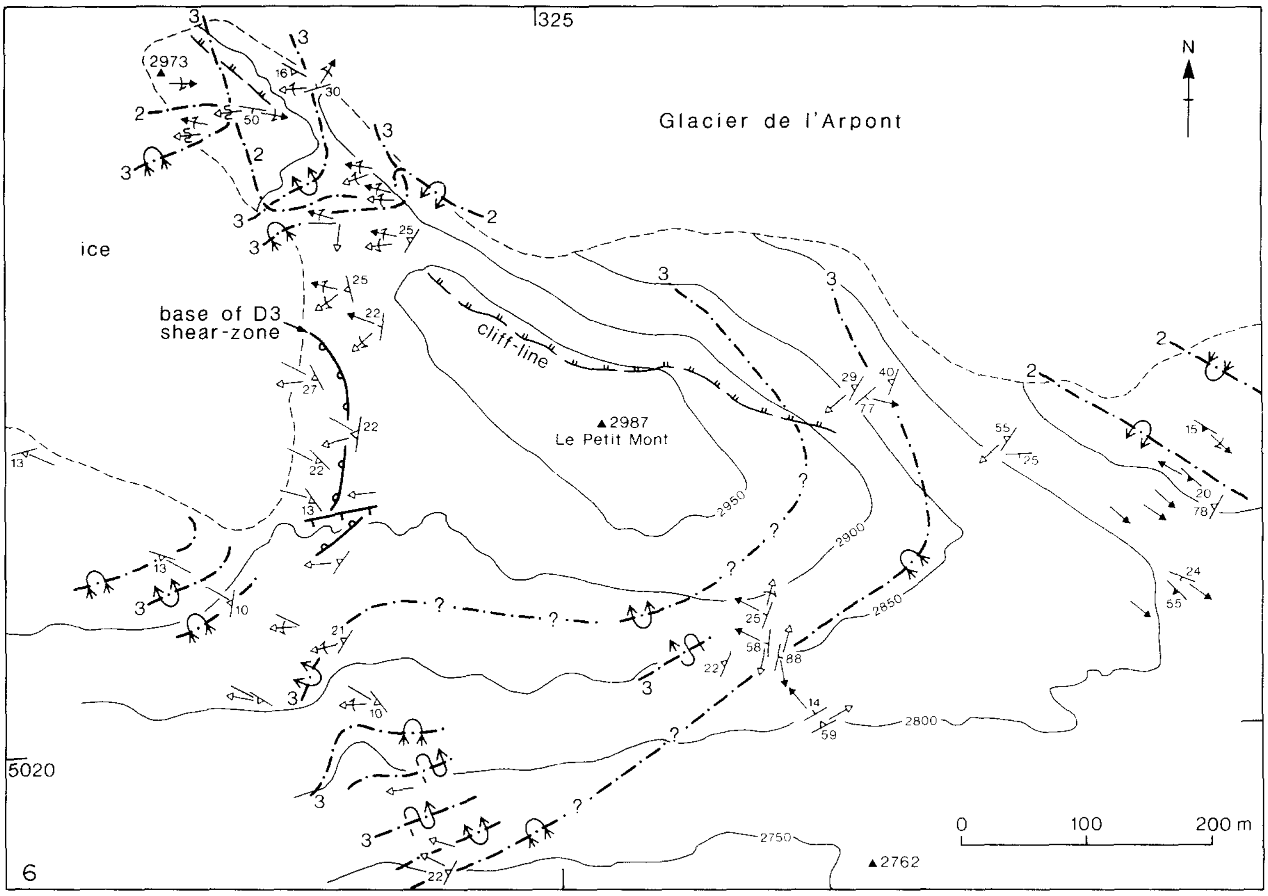

Fig. 6. Structural map of the major D_3 synform in Liassic limestone on Le Petit Mont. For location and symbols see Fig. 3. The half-arrows across fold hinge-lines show the sense of asymmetry (vergence). Major axial traces are numbered by age.

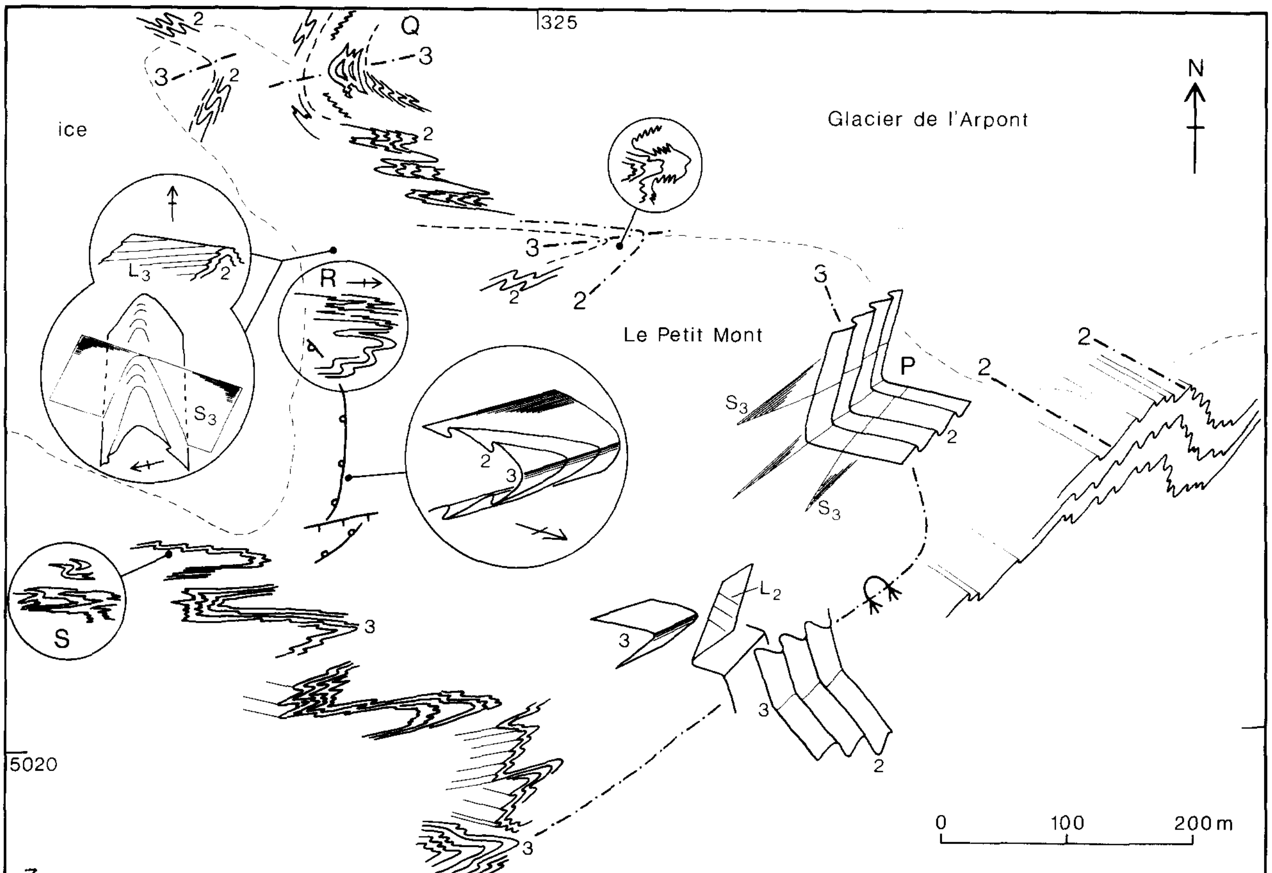

Fig. 7. Cartoon showing the interaction of D_2 and D_3 folds in the area of Fig. 6, superposed on an outline map of the area. Structures not shown as insets are drawn in the correct orientation and at the correct scale (with some poetic licence); those in insets are metre-scale outcrop structures drawn in various orientations, indicated by N-arrows. Structures are numbered by age. P,Q,R,S, locations of sketches and photographs (Figs. 9–12).

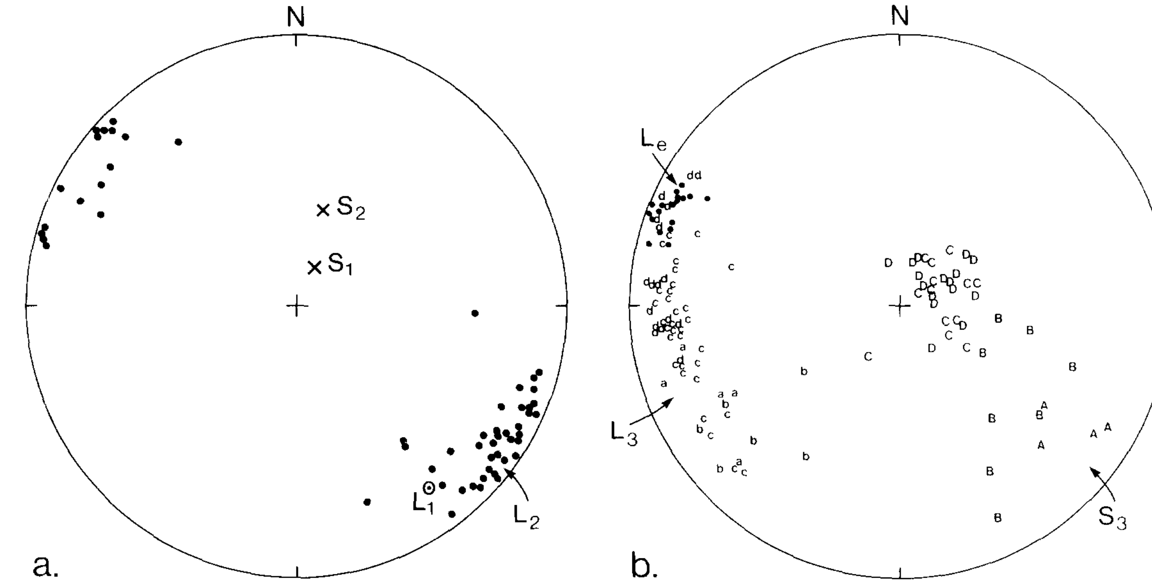

Fig. 8. Orientation data from the Le Petit Mont area. (a) L_2 and small-scale D_2 fold hinges. Means of S_1 and S_2 are shown, and also the mean of 150 glaucophane lineations from the Arpont schist (Platt & Lister 1985) for comparison. (b) Variation in S_3 (capital letters) and L_3 (lower case letters). A, flat limb below lowest D_3 synformal closure (see Figs. 6 and 7); B, lowest D_3 synform; C, between lowest synform and D_3 shear zone (Fig. 6); D, above base of D_3 shear zone. Solid circles, L_e (D_3 elongation lineation.)

d'Amont and parts of the Arpont schist around lac de l'Arpont, D_2 folds are non-cylindrical, trend between SW and W, and have steep S-dipping to vertical axial planes (Fig. 8a). Where D_2 strain is high, as on Le Petit Mont, D_2 folds are highly cylindrical, trend WNW, and have gently S-dipping axial planes. This suggests variably non-coaxial strain during D_2, involving NW–SE shortening combined with a roughly NW-directed sense of shear.

D$_3$ *structures*

The mountain La Dent Parrachée consists of a kilometre scale NE–SW trending synform, overturned towards the SE, that affects the entire nappe pile (Figs. 4c and 9a). Smaller-scale D_3 folds also deform the nappe contacts (Figs. 4d and 5a). The axial trace of the major synform passes through Le Petit Mont (Fig. 6) and Dôme de Chasseforêt in the north of the area. Here, vergence changes of small-scale folds that overprint D_2 structures demonstrate the existence of a complex D_3 synformal closure.

There is a marked gradient in the intensity of deformation across this structure. In the lower, horizontal limb of the major synform on Le Petit Mont the only effect of D_3 deformation is a weak, steeply NW-dipping spaced cleavage, defined by 1–10 cm spaced seams of opaque carbonaceous material concentrated by pressure-solution. Higher up, in the hinge of the lowest D_3 fold (Figs. 6 and 7), this cleavage intensifies abruptly (Fig. 9d), and in addition to pressure-solution seams there are significant effects of intracrystalline plastic deformation in quartz and calcite (undulatory extinction, kinking, and sub-grain formation). Albite porphyroblasts with inclusion trails defining earlier fabrics have been rotated, and they are mantled by carbonaceous material left by pressure-solution of calcite along their boundaries (Fig. 9f). The cleavage dip progressively decreases upwards, until it is nearly horizontal in the hinge of the main D_3 synform. In quartz-rich layers, quartz has been dynamically recrystallized to a grain-size of 20 μm : a substantial reduction from its pre-D_3 grain-size of 150 μm (Fig. 9e). In calcite-rich layers the calcite has taken up the deformation: the grain size

Fig. 9. (a) North face of La Dent Parrachée, looking S. The major D_3 synform dominates the structure, closing in the centre of the face. Triassic dolomite (Td) and Liassic limestone (L) of the Pas Rosset slice occupy the lower limb on the left, and are folded around the synform (see Fig. 4b). Lias, Malm (M) and Cretaceous (C) of the Parrachée nappe in the overturned limb form the summit and northwest ridge (right). (b) Summit and northwest ridge of La Dent Parrachée (looking S), to show isoclinal syncline in Malm and Cretaceous rocks (see Fig. 4b). (c) Spaced S_1 pressure-solution cleavage in Rhaetic limestone. The microstructure has been overgrown helicitically by coarse calcite (note cleavage, lower left) and albite (ab). V295. (d) Broadly spaced S_3 pressure-solution cleavage dips NW (right) in the hinge of the lowest synform on Le Petit Mont (P in Fig. 7). This overprints S_2 (horizontal) defined by quartz lenticles. Lias, looking S. (e) Microstructure of a Liassic quartz–calcite rock from a D_3 shear zone, parallel to the elongation direction. The top half of the field of view is calcite-rich, with dynamically recrystallized calcite showing a moderate shape fabric, and weakly deformed quartz (q). In the quartz-rich lower half, quartz is strongly deformed and extensively recrystallized. V218. (f) Albite porphyroblast with straight inclusions defining S_2 has been rotated during D_3. Albite growth was interkinematic. S_3 (horizontal) is defined by large plastically deformed calcite grains (ca), concentrations of opaque material produced by pressure-solution (particularly around the albite), and by growth fringes of quartz and white mica in the deformation shadows around the albite. Section normal to L_3. V217. Lias.

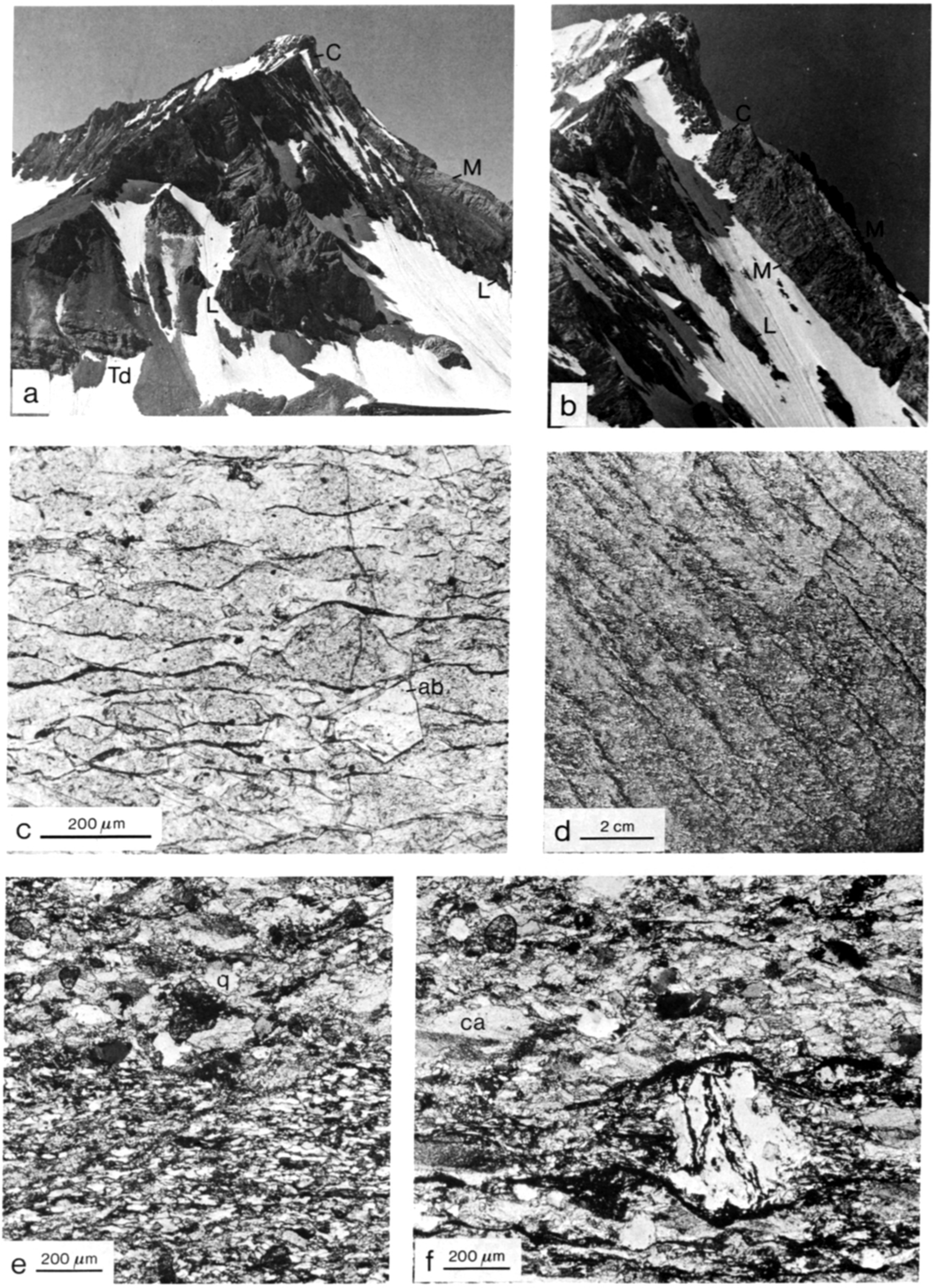

Fig. 9.

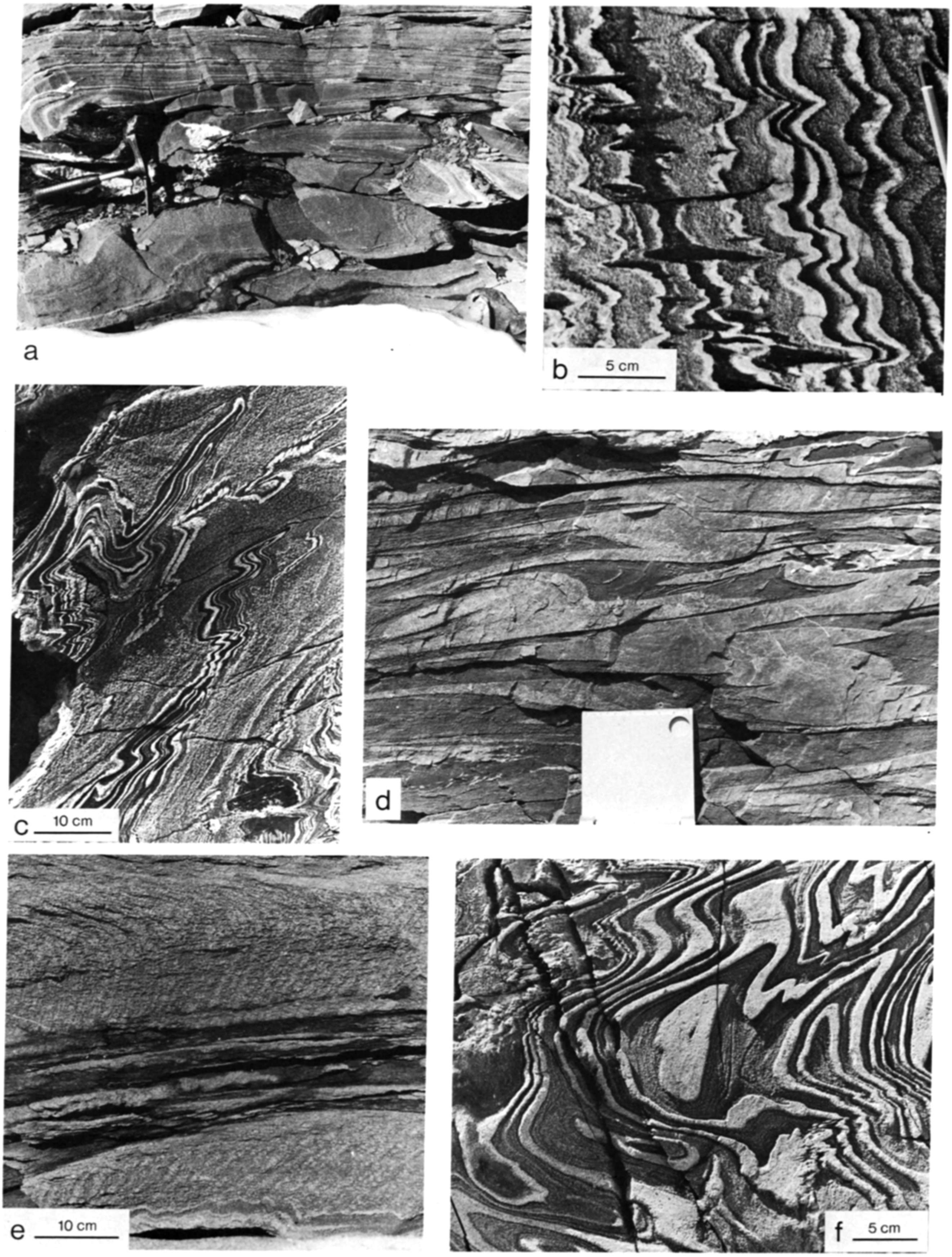

Fig. 10. (a) Lower boundary of the D_3 shear-zone in Lias on Le Petit Mont (R in Fig. 7). Open D_3 folds (bottom left) pass up into isoclinal folds (top right) that transpose the earlier fabrics. Looking SW. See Fig. 11(a). (b) Banded siliceous Liassic limestone, symmetrically folded in D_3 fold hinge (Q in Fig. 7). Small nodules of nearly pure coarse calcite, roughly equant before D_3, have been plastically deformed to higher strains than the surrounding rock (cf. Fig. 10c). Le Petit Mont, looking W. (c) Interference of three sets of folds, locality Q in Fig. 7, looking W. D_1 isoclines are refolded by N-vergent D_2 folds with near-vertical axial-planes (centre left), and nearly symmetrical D_3 folds with horizontal axial-planes are superposed. D_3 strain is fairly low, and the calcite nodules (lower right) have remained nearly undeformed during D_1 and D_2 (cf. Fig. 10b). (d) D_2/D_3 interference structures from the zone of high D_3 strain on Le Petit Mont (S in Fig. 7), looking W. Note that the more competent light-coloured siliceous layers make shapes reminiscent of flying geese, whereas the dark calcareous layers look like vampire bats (cf. Fig. 12). (e) Reversal of cleavage-vergence of S_2 in D_3 shear-zone (R in Fig. 7). Differentiated quartz-calcite foliation S_2 is axial planar to minor N-vergent D_2 folds (bottom), but is folded back towards the SE by D_3 shear (top) without any associated folding of bedding. Looking SW. See Fig. 11b. (f) Spaghetti structure, produced by the interference of D_2 and D_3 folds in the hinge of a major D_3 fold on Le Petit Mont (locality Q, Fig. 7), looking W. Fig. 13 illustrates the evolution of these structures.

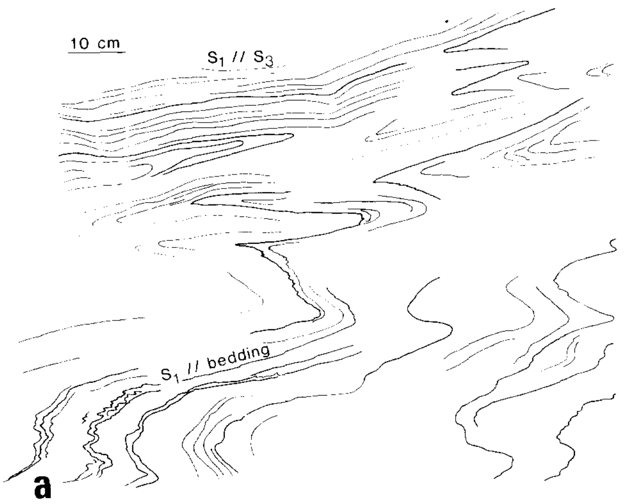

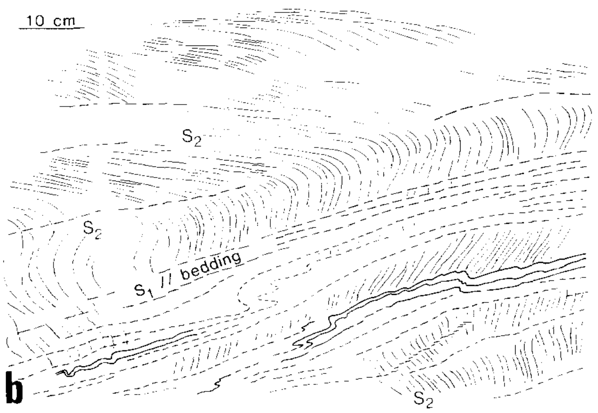

Fig. 11. Structures in the D_3 shear zone on Le Petit Mont (locality S in Fig. 7). (a) D_3 folds increase in tightness on the lower boundary of the shear zone. At the top the older fabric (S_1 parallel to bedding) has been completely transposed into S_3. Looking SW. (b) Folding and reorientation of S_2 independently of bedding, by D_3 shear strain on the lower boundary of the zone. Looking SW. Dashed lines: S_1 parallel to bedding. S_2 is defined by differentiation bands of quartz and calcite in impure Liassic limestone.

produced by dynamic recrystallization is about 50 μm, whereas quartz is virtually undeformed. Nodules of pure coarse-grained calcite in the limestone, which were essentially unaffected by the earlier deformations (Fig. 10c, bottom right) were strongly flattened during D_3 (Fig. 10b). D_3 fold axes and intersection lineations are also reoriented by the increase in D_3 strain. In the lower limb of the synform they trend about 050°, and progressively rotate to about 110° in the axial zone (Figs. 6, 7 and 8b), where they are roughly parallel to a well-marked elongation lineation, defined by the shape of deformed and recrystallized calcite and quartz grains.

The axial zone of the major synform on Le Petit Mont consists of a stack of tight folds (Figs. 6 and 7), with a marked concentration of strain on their overturned limbs. D_3 strain intensity locally changes from nearly zero to very large over distances of 0.5 m (Figs. 10a and 11a); these changes define discrete D_3 shear zones a few metres thick. In the example shown, S_2 is turned back on itself at the margin of the zone, reversing its angular

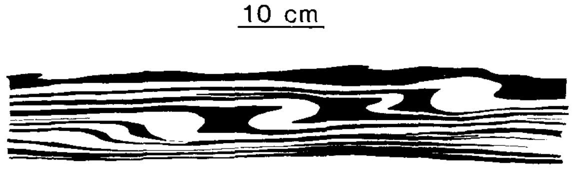

Fig. 12. Flattened buckle folds in the zone of high D_3 strain on Le Petit Mont (locality S in Fig. 7). The rock is composed of alternating bands of micaceous limestone (black) and calcareous quartz schist (white). The folds were probably initiated during D_2. The rounded outer arcs and tightly pinched inner arcs in the siliceous layers suggest that the initial buckling mechanism was controlled by competency contrast, although the folds have been substantially modified by later more homogeneous strain.

relation to bedding (Figs. 10e and 11b). Because D_2 and D_3 fold axes are nearly parallel in the axial zone, they interact to produce what appear to be coaxial interference structures. S_3 dips gently west in this area, whereas D_2 fold axes are nearly horizontal, so L_3 intersection lineations define hairpin loops around D_2 folds (Fig. 7). The initial orientation of the D_3 folds was at a high angle to the D_2 folds, but they have been reoriented by large ductile strain into the D_3 stretching direction, which happened to be roughly parallel to the D_2 fold-axes. As a result, D_2 folds also describe hairpin loops around D_3 closures (Figs. 7 and 13). This has the notable result that the D_2 fold vergence changes around D_3 fold closures, which would not be the case in true coaxial refolding. Because of the strong D_3 stretching, non-linearity of the older fold hinges due to refolding is greatly exaggerated: the axes of the D_1 folds in Fig. 10(e), for example, rotate through large angles around relatively open D_3 warps. D_3 folds themselves also locally rotate within their own axial surfaces through angles of up to 120° to form sheath folds (Cobbold & Quinquis 1980). These effects, involving three sets of folds, produce interference structures of considerable complexity (Figs. 7 and 10c, d, & f).

Three lines of evidence suggests that D_3 deformation was strongly non-coaxial, and allow us to infer a sense of shear. (i) The change of orientation of S_3 with increasing strain (Fig. 8b) suggests SE-directed shear along a roughly horizontal plane. (ii) The strong D_3 stretching lineation trending around 110°, and the reorientation of D_3 folds into this trend, suggests a shear direction slightly south of east. (iii) The reversal of the cleavage-vergence of S_2 in the margin of a D_3 shear zone can only be explained by a strong S- to E-directed component of shear.

Late structures

A characteristic feature of the area is the development of a late extensional crenulation cleavage (Platt & Vissers 1980) in the more schistose rocks. The cleavage clearly postdates D_2 (Platt & Lister 1985), but relations with D_3 are less clear. It is particularly well developed in Permian phyllite involved in zones of D_3 thrusting, suggesting that it may have formed during the later stages of D_3. The sense of shear on the cleavage zones is

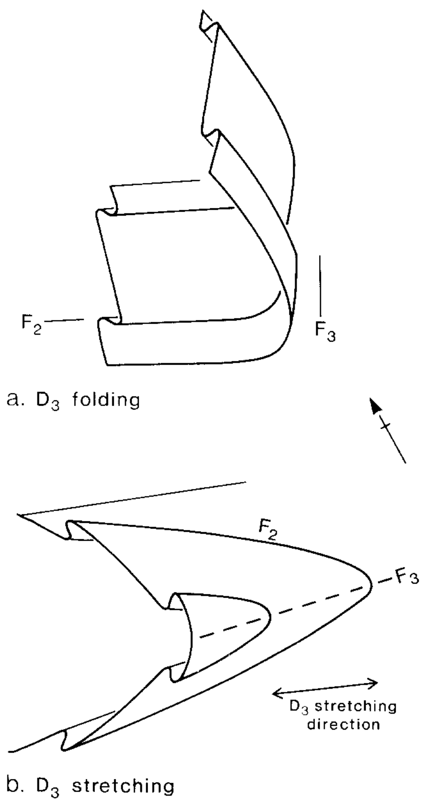

Fig. 13. Evolution of D_2/D_3 fold-interference structures. D_3 fold-hinges (F_3 in diagram) were probably initiated roughly normal to D_2 hinge-lines, so that D_2 vergence changed across D_3 hinges (type 2 of Ramsay 1967). During later D_3 stretching, nearly parallel to the D_2 hinge lines, D_3 folds were rotated close to this orientation. D_2 and D_3 folds are therefore nearly coaxial in zones of high D_3 strain, but D_2 vergence still changes across D_3 hinges.

commonly towards the SE quadrant, which is consistent with this interpretation. It also occurs in the Arpont schist, however, in rocks that have not experienced large D_3 strain. Microstructurally, the cleavage zones are characterized by extensive grain-size reduction of quartz by dynamic recrystallization, and by semi-brittle deformation of mica.

D_3 structures have been folded about N–S trending monoclinal warps that define the culmination of the Vanoise massif. The most important of these is a major downwarp on the western margin of the massif, apparently associated with a zone of late faults (Fig. 1).

TECTONIC SYNTHESIS

The nappe structures

The nappes have been strongly modified by later deformation and they are incompletely preserved, so that our inferences about their origin are necessarily somewhat cautious. The Arpont nappe appears to consist of a disrupted recumbent fold cut by one or more thrusts that have interleaved it with Permian phyllite. The Parrachée nappe and Pas Rosset slice consist of large-scale isoclinal synclines, and the contact between these two may be a faulted-out anticlinal closure. The basal contact of the Parrachée nappe on the Arpont nappe cuts across the axial plane of the major D_1 syncline, suggesting that significant nappe movement occurred during or after folding. Each of these three main nappes therefore consists of a major recumbent fold, which suggests that folding and the accompanying ductile strain were a fundamental part of the nappe-forming process. The NW-trending glaucophane lineation in the Arpont schist probably indicates the tectonic transport direction during at least part of this process. If so, this provides an additional datum in the gradually emerging picture of the kinematics of the Pennine nappes around the Alpine arc (Lacassin 1984, Malavieille & Etchecopar 1981, Savary & Schneider 1983, Steck 1984, Tricart 1984).

It is a reasonable assumption that the nappes were initiated during the major underthrusting event that caused the high-pressure metamorphism, and that significant movement occurred on the nappe contacts at this time. Three lines of evidence, however, suggest that the structures presently visible were formed after underthrusting, and were associated with a later tectonic event that caused significant uplift rather than burial. Firstly, the D_1 structures in the Arpont nappe postdate the high-pressure peak (Platt & Lister 1985). Secondly, the absence of glaucophane and jadeite in any but the Arpont nappe may mean that the rocks in different nappes were metamorphosed at different pressures. This would confirm that the nappes postdate the high P/T event (as has been shown for the upper Penninic and Austro-Alpine nappes of the Zermatt region by Compagnoni *et al.* 1976), and would indicate that some of the nappe contacts (e.g. the Arpont/Parrachée contact) are extensional, in that they have excised part of a depth-related metamorphic zonation. Thirdly, the Arpont/Parrachée nappe contact is clearly extensional with respect to the stratigraphy, in that in places it juxtaposes Liassic rocks directly on Arpont schist. Hence we cannot positively identify any structures in the area as subduction-related, although some of the nappe contacts may have been initiated then and reactivated later.

The nature of this post-subduction tectonic event is unclear, but it undoubtedly involved uplift into a lower pressure metamorphic environment. Overlying material must therefore have been removed, either by erosion, or by horizontal extension and thinning. The extensional geometry of the Arpont/Parrachée nappe contact, in particular, lends some support to the second possibility. Horizontal extension during continental collision seems at first sight somewhat unlikely, but extension driven by the gravitational potential of a major topographic elevation may be accompanying continental collision in the Himalaya and Tibet at the present day (England 1983). A possible unifying model for the early events could therefore involve a phase of subduction and underthrusting that created folds and thrusts and duplicated the stratigraphy (e.g. Pas Rosset slice, Schistes Lustrés nappe), followed by a phase of gravity spreading that caused horizontal extension, flattening of the folds, extensional faults (Arpont/Parrachée nappe contact), and regional uplift as the overburden was extended and thinned. This is comparable to similar models suggested for the central Alps (Milnes 1978), the Scandinavian Caledonides (Williams & Zwart 1977), and the Betic Cordillera (Platt *et al.* 1983). We emphasize, however, that the evidence from the Vanoise does not demonstrate this model conclusively, although it is consistent with it.

From an analytical point of view, we distinguish D_2 as a distinct deformational event. D_2 structures deform D_1 folds and refold nappe contacts, and they formed under distinctly lower-pressure metamorphic conditions than D_1 (Platt & Lister 1985). It is possible, however, that at least some of the structures we call D_2 were a consequence of the later stages of nappe emplacement, although we cannot prove this. Certainly, the D_2 folds beneath Crête des Belles Places and Le Petit Mont (Fig. 4a) do not affect the Arpont/Parrachée nappe contact, implying some displacement on this contact during D_2; and the intensity of D_2 folding in the Arpont schist increases upwards towards this contact. Our inference that D_2 involved NW–SE shortening and NW-directed shear is consistent with the idea that D_1 and D_2 represent a progressive tectonic event.

D_3 clearly refolds the nappe contacts, and is associated with a quite different sense of shear: towards ESE. It is clearly separated in time from D_2 by a static phase of greenschist-facies metamorphism, involving widespread growth of albite porphyroblasts that grew helicitically over earlier fabrics. D_3 appears to be part of the regionally recognized late backfolding and backthrusting event (Debelmas 1976, 1980, Tricart *et al.* 1977, Milnes *et al.* 1981). The major D_3 synform in the area formed beneath a substantial SE-directed thrust that crops out along the western margin of the massif (Figs. 1 and 5b), and carried Permian and younger rocks from the western Vanoise eastwards above the Arpont–Parrachée region. This thrust is particularly well exposed around Tête d'Aussois (UTM 3198,0181, unpublished work by F. Peel), and in Fig. 1 we show how it may link with related major structures in the Vanoise.

D_3 postdates the peak of the greenschist metamorphism. If, as we suggest, the latter correlates with the end-Eocene Lepontine event in the central Alps, then D_3 is Oligocene or younger. It may therefore be related to regional horizontal compression caused by the emplacement of the Penninic allochthon as a whole onto the European continental margin in Oligocene time. The microstructural evidence for the importance of the relatively high-stress deformational mechanism of intracrystalline plasticity during this event is consistent with this interpretation. We note, however, that 'backthrusting' events in the Alps are not necessarily synchronous, nor need they have the same cause. They appear to become progressively younger towards the outside of the Alpine arc (Tricart 1984), and the sense of movement changes from SE in the Swiss Alps (Savary & Schneider 1983), to ESE in the Vanoise, and to NE in the southwestern Alps (Tricart 1984).

CONCLUSIONS

Several distinct stages in the tectonic evolution of the Arpont–Parrachée area can be recognized. High-pressure metamorphism in the Arpont schist was caused by deep tectonic burial during subduction or collision, but we cannot confidently identify structures directly related to this event. The main phase of nappe formation involved isoclinal folding on both large and small scales, as well as major displacements, probably to the NW, on discrete flat-lying fault zones, one of which has an extensional geometry. The associated ductile deformation postdated the peak of the high-pressure metamorphism, and this tectonic event appears to be primarily related to the uplift history of the rocks. Roughly E–W trending D_2 folds form a distinct set of structures, and were associated with lower greenschist-facies metamorphism. It is nevertheless possible that D_2 structures were produced during the final stages of nappe emplacement. Pressure-solution was an important deformational mechanism during both D_1 and D_2. D_2 was followed by a middle greenschist facies static thermal peak, which separated it in time from D_3. The latter caused large- and small-scale folds, overturned towards the SE, accompanied and followed by localization of deformation into ESE-directed shear zones and thrusts, rotation of fold axes, and formation of widespread extensional crenulation cleavage. The dominant deformational mechanism was intracrystalline plasticity in quartz and calcite.

Acknowledgements—We are grateful to Jacqueline Desmons, Reinoud Vissers, Hervé Dondey and Frank Peel for discussion of problems in the field and on paper, to Jacques Dorleijn for contributing field and structural data from the Plan d'Amont area, and to the anonymous referees for their helpful and encouraging comments. Clare Pope and Richard Macavoy helped with draughting and photography. And thanks to Janos Urai for pulling JPP up that mountain!

REFERENCES

Bocquet, J. 1974a. Études minéralogiques et pétrologiques sur les métamorphismes d'âge alpin dans les alpes françaises. Thesis. University of Grenoble.

Bocquet, J. 1974b. Le socle briançonnais de Vanoise (Savoie): arguments en faveur de son âge anté-alpin et son polymétamorphisme. *C. r. hebd. Séanc. Acad. Sci., Paris* **178D**, 2601–2604.

Bocquet, J., Delaloye, M., Hunziker, J. C. & Krummenacher, D. 1974. K–Ar and Rb–Sr dating of blue amphiboles, micas, and associated minerals from the western Alps. *Contr. Miner. Petrol.* **47**, 7–26.

Caby, R., Kienast, J-R. & Saliot, P. 1978. Structure, métamorphisme et modéle d'évolution tectonique des Alpes Occidentales. *Revue Géogr. phys. Géol. dyn.* **20**, 307–322.

Cobbold, P. R. & Quinquis, H. 1980. Development of sheath folds in shear regimes. *J. Struct. Geol.* **2**, 119–126.

Compagnoni, R., Dal Piaz, G. V., Hunziker, J. C., Gosso, G., Lombardo, B. & Williams, P. F. 1976. The Sesia–Lanzo Zone, a slice of continental crust with Alpine high-pressure low-temperature assemblages in the Western Italian Alps. In: *High Pressure–Low Temperature Metamorphism of the Oceanic and Continental Crust in the Western Alps*. Consiglio Nazionale Richerche, Torino, 123–176.

Debelmas, J. 1974. *Géologie de France*. Doin.

Debelmas, J. 1976. Deux coupes transversales des Alpes franco-italiennes. *Schweiz. Miner. Petrogr. Mitt.* **56**, 561–565.

Debelmas, J. & Lemoine, 1970. The Western Alps: palaeogeography and structure. *Earth Sci. Rev.* **6**, 221–256.

Debelmas, J. & Kerckhove, C. 1980. Les Alpes franco-italiennes. *Géol. Alpine* **56**, 21–58.

Desmonds, J. 1977. Mineralogical and petrological investigations of alpine metamorphism in the internal French Western Alps. *Am. J. Sci.* **277**, 1045–1066.

Ellenberger, F. 1958. *Étude géologique du pays de Vanoise*. Mémoir explicative de la Carte géologique de France. *Mem. Bur. Rech. géol. min. Fr.* **15**.

Ellenberger, F. 1960. Sur une paragénèse éphémère à lawsonite et glaucophane dans le métamorphisme alpin en Haute-Maurienne (Savoie) *Bull. soc. géol. Fr.* 7 *Ser.* **9**, 190–194.

Ellenberger, F. 1966. Le Permien du Pays Vanoise. In: *Atti del Symposium sul Verrucano Pisa, settembre 1965*. Soc. Toscana di Scienze Naturali, Pisa, 170–211.

England, P. 1983. Some numerical investigations of large-scale continental deformation. In: *Mountain Building Processes* (edited by Hsü, K. J.). Academic Press New York, 129–139.

Frey, M., Hunziker, J. C., O'Neil, J. R. & Schwander, H. W. 1976. Equilibrium–disequilibrium relations in the Monte Rosa granite, western Alps: petrological, Rb–Sr and stable isotope data. *Contr. Miner. Petrol.* **55**, 147–179.

Frisch, W. 1979. Tectonic progradation and plate tectonic evolution of the Alps. *Tectonophysics* **60**, 121–139.

Goffé, B. 1977. Succession de subfacies métamorphiques en Vanoise méridionale (Savoie). *Contr. Miner. Petrol.* **62**, 23–42.

Goffé, B. 1982. Definition du faciès à Fe,Mg-carpholite–chloritoïde, un marquer du métamorphisme de HP–BT dans les métasediments alumineux. *Mem. Sci. Terre Univ. Curie*, Paris.

Goffé, B., Goffé-Urbano, G. & Saliot, P. 1973. Sur la présence d'une varieté magnésienne de ferrocarpholite en Vanoise (Alpes françaises). Sa signification probable dans le métamorphisme alpin. *C. r. hebd. Séanc. Acad. Sci., Paris* **277D**, 1965–1968.

Homewood, P., Gosso, G., Escher, A. & Milnes, A. G. 1979. Cretaceous and Tertiary evolution along the Besançon–Biella traverse (Western Alps). *Eclog. geol. Helv.* **73**, 635–649.

Lacassin, R. 1984. Cisaillement ductile et déformation hétérogène du granite de la nappe du Mont-Rose dans la vallée de Saas (Suisse). *C. r. hebd. Séanc. Acad. Sci., Paris* **296**, 777–782.

Malavieille, J. & Etchecopar, A. 1981. Ductile shear deformation of quartzite in an Alpine crustal thrust (Ambin massif). *Tectonophysics* **78**, 65–71.

Milnes, A. G. 1978. Structural zones and continental collision, Central Alps. *Tectonophysics* **47**, 369–392.

Milnes, A. G., Greller, M. & Müller, R. 1981. Sequence and style of major post-nappe structures, Simplon–Pennine Alps. *J. Struct. Geol.* **3**, 411–420.

Platt, J. P. & Lister, G. S. 1978. Déformation, métamorphisme et mécanismes d'écoulement dans le massif de la Vanoise, Alpes penniques françaises. *C. r. hebd. Séanc. Acad. Sci.* **287D**, 895–898.

Platt, J. P. and Lister, G. S. 1985. Structural history of high-pressure metamorphic rocks in the southern Vanoise massif, French Alps, and their relation to Alpine tectonic events. *J. Struct. Geol.* **7**, 19–35.

Platt, J. P., van den Eeckhout, B., Janzen, E., Konert, G., Simon, O. J., and Weijermars, R. 1983. The structure and tectonic evolution of the Aguilón fold-nappe, Sierra Alhamilla, Betic Cordilleras, SE Spain. *J. Struct. Geol.* **5**, 519–538.

Platt, J. P. & Vissers, R. L. M. 1980. Extensional structures in anisotropic rocks. *J. Struct. Geol.* **2**, 387–410.

Ramsay, J. G. 1967. *Folding and Fracturing of Rocks*. McGraw-Hill, New York.

Raoult, J. F. 1980. Interprétation nouvelle de la Vanoise (zone briançonnaise, Alpes françaises). *Revue Géogr. phys. Géol. dyn.* **22**, 303–312.

Savary, J. & Schneider, B. 1983. Déformations superposées dans les Schistes lustrés et les ophiolites du val d'Herens (Valais). *Eclog. geol. Helv.* **76**, 381–389.

Steck, A. 1984. Structures de déformations tertiaires dans les Alpes centrales. *Eclog. geol. Helv.* **77**, 55–100.

Tricart, P., Caron, J-M, Gay, M. & Vialon, P. 1977. Relais de schistosités, structures en éventail et discontinuitiés majeures sur la transversale du Pelvoux (Alpes occidentales). In: *Alpes, Appennins, Hellénides. Bull. soc. géol. Fr.* **14**, 873–881.

Tricart, P. 1984. From passive margin to continental collision: a tectonic scenario for the Western Alps. *Am. J. Sci.* **284**, 97–120.

Trümpy, R. 1960. Palaeotectonic evolution of the central and Western Alps. *Bull. geol. Soc. Am.* **71**, 843–908.

Trümpy, R. 1980. *Geology of Switzerland*. Wepf & Co., Basel.

Williams, P. F. & Zwart, H. J. 1977. A model for the development of the Seve–Köli Caledonian nappe complex. In: *Energetics of Geological Processes* (edited by Saxena, S. K. & Bhattacharji, S.), Springer, Berlin.